

# Determining the terahertz optical properties of subwavelength films using semiconductor surface plasmons

T. H. Isaac,<sup>a)</sup> W. L. Barnes, and E. Hendry

*School of Physics, University of Exeter, Stocker Road, Exeter EX4 4QL, United Kingdom*

(Received 22 August 2008; accepted 15 November 2008; published online 19 December 2008)

By employing a combination of time-domain measurements and numerical calculations, we demonstrate that the semiconductor InSb supports a strongly confined surface plasmon (SP) in the terahertz frequency range. We show that these SPs can be used to enhance the light-matter interaction with dielectric layers above the semiconductor surface, thereby allowing us to detect the presence of polystyrene layers around 1000 times thinner than the free space wavelength of the terahertz light. Finally we discuss the viability of using semiconductor SPs for the purposes of terahertz sensing and spectroscopy. © 2008 American Institute of Physics.

[DOI: 10.1063/1.3049350]

Due to its nonionizing nature and the distinctive optical response of many molecules in the terahertz frequency range, there has been much recent interest in using terahertz radiation for chemical and biological analysis.<sup>1-3</sup> However, with terahertz wavelengths ranging from 100 to 1000  $\mu\text{m}$ , the diffraction limit for this long wavelength light means that it is difficult to measure small volume samples. Recent work<sup>4-6</sup> has demonstrated that by propagating terahertz radiation along a metallic surface or waveguide it is possible to detect the presence of thin dielectric layers on the metal surface by allowing the terahertz surface wave to traverse a greater length of analyte. The effectiveness of this type of measurement geometry has recently been demonstrated by the development of a terahertz biosensor for DNA binding.<sup>7</sup>

Near the surface plasma frequency of a conductor (typically in the UV/visible spectral region for most metals) a propagating surface plasmon (SP) can exhibit subwavelength confinement of electric field in the direction normal to a conductor-dielectric interface.<sup>8</sup> This subwavelength field distribution enhances light-matter interactions with material in the region above the conductor surface—a property which has been utilized in the development of SP biosensors.<sup>9,10</sup> In contrast, at frequencies well below the metal plasma frequency, SPs exhibit very weak field confinement.<sup>11</sup> Semiconductors, on the other hand, exhibit a plasma frequency that depends on the conduction band electron density, so that the properties of semiconductor SPs can be tailored within the terahertz frequency range through doping<sup>12</sup> and photoexcitation.<sup>13</sup> In particular, narrow gap semiconductors such as InSb have an intrinsic electron density appropriate for supporting low loss, highly confined terahertz SPs at room temperature.<sup>14,15</sup> Indeed, the dielectric function of InSb in the terahertz frequency range<sup>14</sup> is remarkably similar to that of plasmon supporting metals such as gold and silver in the UV/visible frequency range.<sup>16</sup>

In this paper we present phase-resolved measurements which demonstrate that it is possible to determine the optical properties of a submicron sized dielectric layer above an InSb surface using a propagating SP. We show that the SP on InSb is significantly more sensitive to the dielectric layer than surface modes supported on a gold substrate. Moreover,

we show that the sensitivity to the dielectric analyte increases significantly as one approaches the surface plasma frequency of InSb. We discuss potential applications of terahertz semiconductor SPs for the measurement of analytes of subwavelength dimensions.

We use the Drude model to approximate the dielectric function of the conductors (gold and InSb) in the terahertz frequency range,

$$\varepsilon_c(\omega) = \varepsilon_{\text{lattice}} - \frac{\omega_p^2}{\omega^2 + i\omega\gamma}. \quad (1)$$

For gold, we use a plasma frequency  $\omega_p$  of  $1.2 \times 10^{16}$  rad/s and a scattering rate  $\gamma$  of  $1.2 \times 10^{14}$  rad/s. These values are fitted from visible/IR data from Ref. 16. The lattice permittivity  $\varepsilon_{\text{lattice}}$  of gold is taken<sup>17</sup> to be 9.1. At terahertz frequencies the permittivity of gold is very large<sup>18</sup> and predominantly imaginary ( $\varepsilon_c = -1.0 \times 10^4 + 1.6 \times 10^6 i$  at 1.2 THz), so that the terahertz surface electromagnetic mode is only weakly bound. Using the Drude parameters above, we calculate<sup>8</sup> that at 1.2 THz the decay length for the surface mode electric field into air above a gold substrate is expected to be 1.8 cm [see Fig. 1(a)]. For InSb we use<sup>19</sup>  $\varepsilon_{\text{lattice}} = 15.6$  and Drude parameters<sup>14</sup> are  $\omega_p = 46 \times 10^{12}$  rad/s and  $\gamma = 0.3 \times 10^{12}$  rad/s. Drude parameters will vary considerably between samples of semiconductor owing to variations in impurity density. In this work we use parameters found to be accurate for previous work on InSb samples from the same

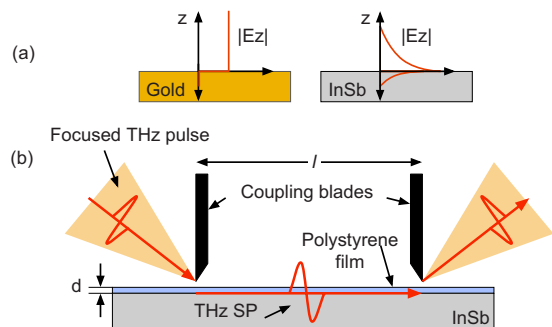


FIG. 1. (Color online) (a) The electric field associated with a SP on InSb is much more strongly confined to the surface than for the terahertz frequency surface eigenmode on gold. (b) Diagram of the measurement geometry.

<sup>a)</sup>Electronic mail: t.isaac@ex.ac.uk.

wafers (Ref. 14), which have a specified dc conductivity at 77 K of  $2400 \text{ S m}^{-1}$ .

The surface plasma frequency<sup>20</sup>  $\omega_{\text{SP}}$  (defined as the high-frequency cutoff for a SP propagating on a conductor-air interface), occurring when the real part of  $\epsilon_c$  is  $-1$ , is approximately 1.7 THz in InSb.<sup>14</sup> Near  $\omega_{\text{SP}}$ , the electric field associated with the SP decays very quickly into the dielectric region above the surface [Fig. 1(a)]: in contrast to gold, the SP propagating on an InSb-air interface at 1.2 THz has a decay length into the air of only  $178 \mu\text{m}$ , less than 70% of the wavelength of free space radiation and two orders of magnitude smaller than the decay length for the surface mode on gold. We show below that this strong confinement of the electric field near the InSb surface enhances the light-matter interaction in the region near the surface. The imaginary component of InSb dielectric function is low throughout the terahertz range, resulting in a long propagation length<sup>20</sup> for the SP.

We spin coat gold and InSb substrates with thin layers of polystyrene from a solution in methoxybenzene. The layer thickness is measured using a surface profiler. We determine the dispersion of the surface modes using a terahertz time-domain spectrometer (with bandwidth of 0.2–2 THz) similar to that described in Ref. 14, flushed with dry air to minimize absorption of the terahertz radiation by water. A schematic of the measurement geometry is shown as in Fig. 1(b). In our experiment we couple to the surface modes on the coated gold and InSb substrates by scattering a focused TM polarized terahertz pulse through a  $300 \mu\text{m}$  wide slit aperture formed between the InSb surface and a steel blade. Using a second blade aperture placed 1 cm along the surface from the input coupling blade, we couple the surface mode back to freely propagating radiation, which is then measured in the far field. Time-domain electric field profiles of transmitted terahertz pulses are converted by means of a fast Fourier transform to complex transmission spectra  $A(\omega)e^{i\phi(\omega)}$ , containing both the amplitude  $A$  and phase  $\phi$  of each frequency component. Normalizing these transmission spectra against a reference spectrum (i.e., of a substrate without dielectric layer) yields the analyte-induced change in phase across the sample,  $\Delta\phi$ . This corresponds to a change in wave number given by  $\Delta k = \Delta\phi/l$ , where  $l$  is the propagation length between the blades (1 cm). The size of phase shift measured is determined by the distance which the SP propagates through the analyte, while the upper limit of the measurable frequency range is determined by the propagation length of the SP upon approaching  $\omega_{\text{SP}}$ . The propagation length of 1 cm is chosen such that the size of phase shift at frequencies below the upper limit is measurable for the thinnest polymer films, while simultaneously ensuring that the upper limit is well into the terahertz frequency range.

In Fig. 2 the data points represent  $\Delta k$  measured for several thicknesses of polymer layer on InSb [Fig. 2(a)] and gold [Fig. 2(b)] substrates, respectively. First, as expected, the phase shifts are larger for thicker polymer films. The measured wave number shifts for polymer covered InSb substrates are clearly larger than for the gold substrates. Furthermore, for the InSb samples we can see a clear trend with  $\Delta k$  increasing considerably as approaching the surface plasma frequency of the InSb. At 1.2 THz  $\Delta k$  is typically twice as large as those for a similar polymer film on the gold substrate.

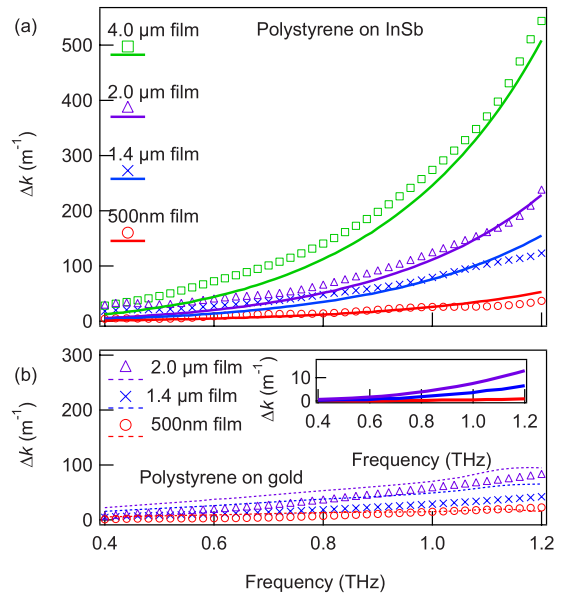


FIG. 2. (Color online) (a) The measured change in dispersion (symbols) of a SP on an InSb substrate induced by various thicknesses of polystyrene. Solid lines indicate the results of analytical modeling. The dispersion shift increases rapidly as the excitation frequency approaches the surface plasma frequency (at 1.7 THz). Measurement bandwidth is limited to 1.2 THz by the propagation length of the SP. (b) Equivalent results for a gold substrate. Dashed lines are the results of finite element modeling of the system that includes the effects of input and output coupling blade apertures. Inset: analytical modeling for the gold substrate underestimates the change in dispersion by almost an order of magnitude.

It is possible to determine the wave number of the SP mode for such a three-layer system<sup>21</sup> analytically through the solution of the simple expression found in Eq. (12) of Ref. 22. Taking this expression we find the SP wave number ( $k$ ) using the Drude model for the permittivity of the conductor. We then normalize the wave number in the same manner as the experiment, i.e., we find  $\Delta k = k_{\text{poly}} - k_{\text{air}}$ , where  $k_{\text{air}}$  is the wave number of a SP on an uncoated substrate and  $k_{\text{poly}}$  is the wave number with a dielectric coating. The best fits as determined by a minimization of the least-squares errors between experiment and analytical solution are plotted as solid lines in Fig. 2(a). Fits are restricted to polystyrene permittivities in the range of  $2.5 \leq \epsilon_p \leq 3.5$ . For InSb substrates, the calculated and measured wave number changes agree fairly well with a dielectric constant of the polystyrene layer of  $\epsilon_p = 2.9 \pm 0.2$ . The maximum deviation between experimental results and the fits is  $35 \text{ m}^{-1}$  on the  $4 \mu\text{m}$  film at 1.2 THz. By analyzing the spectral amplitude of the experimental signal with the loss predicted by the analytical model, we ascertain that for this material, the imaginary component of  $\epsilon_p$  is negligible ( $< 0.1$ ) in the terahertz frequency range. The value of  $\epsilon_p$  and the absence of absorption found from these fits agree with the results of direct terahertz transmission measurements on 2 mm thick samples of polystyrene.

The results of the analytical model for polystyrene layers on gold substrates are plotted in the inset of Fig. 2(b); the calculated shifts are more than an order of magnitude smaller than those found for the InSb substrate in Fig. 2(a). This highlights the greater sensitivity to dielectric analyte expected for a SP on InSb compared to the surface eigenmode on gold. However, it should be noted that the shifts in wave number that we find from our measurements on gold [main panel of Fig. 2(b)] are considerably larger than those pre-

dicted by the analytical model [inset in Fig. 2(b)]. This suggests that for the gold substrates, we do not experimentally interrogate the eigenmode of the system. Indeed, this is clear when we consider the length scales involved in the experiment: since the electric field of the eigenmode is expected to decay over several centimeters in the direction normal to the surface, we will not excite the gold surface eigenmode over the finite lateral propagation length (1 cm) from our small coupling aperture (300  $\mu\text{m}$ ). Contrary to previous claims,<sup>5</sup> the terahertz aperture coupling technique as presented here and elsewhere<sup>23</sup> will not, therefore, interrogate the SP mode of a planar metal surface. Instead, the measurement will be very sensitive to the phase of the diffracted field from our input-coupling aperture. In order to properly simulate the complete system including the coupling elements, we carry out a full finite element method numerical model.<sup>24</sup> In order to reduce computational overheads the model is approximated to be semi-infinite in the plane orthogonal to the propagation direction [i.e., into the plane of the page of Fig. 1(b)]. While computationally demanding, the results of this numerical model [dashed lines in Fig. 2(b)] are much closer to our measured gold data than the analytical solution. The largest deviation between model and experiment is of size  $65\text{ m}^{-1}$ . We find that the numerical model is very sensitive to the precise size and shape of the coupling apertures; we therefore attribute the remaining discrepancies between the numerical model and data to the limited precision with which the experimental configuration can be reproduced in our computer model. On the other hand, analytical modeling is clearly adequate to reproduce the measured phase shifts induced in the surface eigenmode on an InSb substrate. For these substrates, the confinement of SP electric field on InSb (decay length<sup>20</sup> of 178  $\mu\text{m}$  at 1.2 THz) means that the scattered radiation from the input coupling aperture can efficiently couple well to the surface eigenmode within the 1 cm propagation distance of our experiment.

The aperture coupling technique that we employ here allows the interrogation of terahertz optical properties over a broad frequency range using a simple analytical formula for evaluation. By combining both amplitude and phase measurements, a complete characterization of the optical properties of other analytes, such as those of interest in biological or chemical studies, is therefore possible. Biological analytes, which typically contain water and other polar molecules, are generally characterized by terahertz dielectric functions with a large imaginary component (for example, the imaginary component of the permittivity of bulk water<sup>25</sup> at 1 THz is approximately 9.80). Using our analytical model, we can evaluate the effects of an absorbing analyte by finding the wave number and propagation length for a 500 nm analyte layer with dielectric function of  $\epsilon_p = 2.9 + 5i$ . The results of these calculations indicate only a slight increase in the wave number shift above that for a nonabsorbing analyte. More interestingly, an absorbing dielectric layer will lead to a significant drop in the propagation length of the SP. The drop in propagation length is calculated to be between 15% (at 0.4 THz) and 28% (at 1.2 THz)—the drop in propagation length increases approaching the surface plasma frequency

of InSb. An absorbing analyte will therefore be more readily identified (and in smaller volumes) than a nonabsorbing analyte; further calculations indicate that a film of absorbing analyte as thin as 50 nm will induce a readily measurable change in propagation length of 4.8% at 1.2 THz.

In conclusion, our results demonstrate that it is possible to use semiconductor SPs to interrogate the terahertz optical properties of thin film analytes. We show that it is possible to measure the dielectric properties of low index films of thickness almost three orders of magnitude smaller than the wavelength of freely propagating radiation. We show that by combining the amplitude and phase information in a measurement, the complete dielectric response of such a thin film can be extracted from simple analytical formulations.

T.H.I. and E.H. acknowledge the support of the EPSRC-GB (UK). E.H. also acknowledges the RCUK (UK). W.L.B. acknowledges the support of a Wolfson Royal Society Merit award.

<sup>1</sup>P. C. Upadhyaya, Y. C. Shen, A. G. Davies, and E. H. Linfield, *Vib. Spectrosc.* **35**, 139 (2004).

<sup>2</sup>L. L. Van Zandt and V. K. Saxena, *Phys. Rev. A* **39**, 2672 (1989).

<sup>3</sup>T. Ikeda, A. Matsushita, M. Tatsuno, Y. Minami, M. Yamaguchi, K. Yamamoto, M. Tani, and M. Hangyo, *Appl. Phys. Lett.* **87**, 034105 (2005).

<sup>4</sup>J. Zhang and D. Grischkowsky, *Opt. Lett.* **29**, 1617 (2004).

<sup>5</sup>J. Saxler, J. Gómez Rivas, C. Janke, H. P. M. Pellemans, P. Haring Bolívar, and H. Kurz, *Phys. Rev. B* **69**, 155427 (2004).

<sup>6</sup>J. Cunningham, C. Wood, A. G. Davies, C. K. Tiang, P. Tosch, D. A. Evans, E. H. Linfield, I. C. Hunter, and M. Missous, *Appl. Phys. Lett.* **88**, 071112 (2006).

<sup>7</sup>M. Nagel, F. Richter, P. Haring Bolívar, and H. Kurz, *Phys. Med. Biol.* **48**, 3625 (2003).

<sup>8</sup>W. L. Barnes, *J. Opt. A, Pure Appl. Opt.* **8**, S87 (2006).

<sup>9</sup>C. E. Stewart, I. R. Hooper, and J. R. Sambles, *J. Phys. D* **41**, 105408 (2008).

<sup>10</sup>J. G. Gordon II and J. D. Swalen, *Opt. Commun.* **22**, 374 (1977).

<sup>11</sup>A. P. Hibbins, M. J. Lockyear, I. R. Hooper, and J. R. Sambles, *Phys. Rev. Lett.* **96**, 073904 (2006).

<sup>12</sup>J. Gómez Rivas, M. Kuttge, P. Haring Bolívar, H. Kurz, and J. A. Sánchez-Gil, *Phys. Rev. Lett.* **93**, 256804 (2004).

<sup>13</sup>E. Hendry, F. J. Garcia-Vidal, L. Martín-Moreno, J. Gómez Rivas, M. Bonn, A. P. Hibbins, and M. J. Lockyear, *Phys. Rev. Lett.* **100**, 123901 (2008).

<sup>14</sup>T. H. Isaac, J. Gómez Rivas, J. R. Sambles, W. L. Barnes, and E. Hendry, *Phys. Rev. B* **77**, 113411 (2008).

<sup>15</sup>R. Parthasarathy, A. Bykhovski, B. Gelmont, T. Globus, N. Swami, and D. Woolard, *Phys. Rev. Lett.* **98**, 153906 (2007).

<sup>16</sup>*Handbook of Optical Constants of Solids*, edited by E. D. Palik (Academic, New York, 1985).

<sup>17</sup>A. Vial, A.-S. Grimault, D. Macías, D. Barchiesi, and M. L. de la Chapelle, *Phys. Rev. B* **71**, 085416 (2005).

<sup>18</sup>H. Yasuda and I. Hosako, *IEEE/MTT-S Int. Microwave Symp. Dig.*, 3–8 June 2007, 1125 (2007).

<sup>19</sup>S. C. Howells and L. A. Schlie, *Appl. Phys. Lett.* **69**, 550 (1996).

<sup>20</sup>H. Raether, *Surface Plasmons on Smooth and Rough Surfaces and on Gratings* (Springer, Berlin, 1988).

<sup>21</sup>P. K. Tien, *Rev. Mod. Phys.* **49**, 361 (1977).

<sup>22</sup>F. Yang, J. R. Sambles, and G. W. Bradberry, *Phys. Rev. B* **44**, 5855 (1991).

<sup>23</sup>S. A. Maier and S. R. Andrews, *Appl. Phys. Lett.* **88**, 251120 (2006).

<sup>24</sup>HFSS, Version 10, Ansoft Corporation, Pittsburgh, 2006.

<sup>25</sup>L. Thrane, R. H. Jacobsen, P. Uhd Jepsen, and S. R. Keiding, *Chem. Phys. Lett.* **240**, 330 (1995).